Photovoltaic chiral magnetic effect in Weyl semimetals

Katsuhisa Taguchi, Tatsushi Imaeda, Masatoshi Sato, and Yukio Tanaka

Photovoltaic chiral magnetic effect in Weyl semimetals

Katsuhisa Taguchi[1,3], Tatsushi Imaeda[1,3], Masatoshi Sato[2,3], and Yukio Tanaka[1,3]

[1] *Department of Applied Physics, Nagoya University, Nagoya, 464-8603, Japan*

[2] *Yukawa Institute for Theoretical Physics, Kyoto University, Kyoto, 606-8502, Japan*

[3] *CREST, Japan Science and Technology Corporation (JST), Nagoya 464-8603, Japan*

(Dated: April 21, 2016)

We theoretically predict current generation in Weyl semimetals when circularly polarized light is applied. The electric field of the light can drive an effective magnetic field on the order of 10 T. For lower-frequency light, a nonequilibrium spin distribution is formed near the Fermi surface. Spin–momentum locking induces a giant electric current proportional to the effective magnetic field. In contrast, higher-frequency light realizes a quasi-static Floquet state with no induced electric current. We discuss the relevant materials and estimate the order of magnitude of the induced current.

Introduction— Dirac and Weyl semimetals, which host bulk gapless excitations obeying quasi-relativistic fermion equations, have attracted much attention recently in condensed matter physics [1–15]. Dirac semimetals have been theoretically predicted [1–3] and experimentally demonstrated in $(Bi_{1-x}In_x)_2Se_3$ [4, 5], Na_3Bi [6, 7], Cd_3As_2 [8, 9], and $TlBiSSe$ [9, 10]. Several experiments also support the realization of Weyl semimetals in TaAs [11–14]. Moreover, Dirac and Weyl semimetals have been theoretically predicted in a superlattice heterostructure consisting of a topological insulator/normal insulator [3], and a Dirac semimetal has been realized in the $GeTe/Sb_2Te_3$ superlattice [15].

Low-energy bulk excitations in Dirac and Weyl semimetals come in pairs of left- and right-handed Weyl fermions, as described by Nielsen and Ninomiya's no-go theorem [16]. In the low-energy limit, each charge flow of left- and right-handed Weyl fermions is preserved classically, but their difference, the axial current, is not conserved in quantum theory owing to the chiral anomaly. In an analogy with relativistic high-energy physics [17–22], the anomaly-related effects have been discussed in condensed matter physics [23–32]. The anomaly-induced currents are dissipationless; thus, they have potential applications to unique electronics.

Among the anomaly-related effects, one of the most interesting phenomena is the chiral magnetic effect. In the presence of a time-dependent θ term in the Dirac–Weyl theory, a current proportional to an applied static magnetic field has been predicted theoretically [17–21, 24–27]. The flow due to the static magnetic field, however, might be problematic in condensed matter physics. First, in Weyl semimetals, the time-dependent θ term is obtained in the ground state, in the presence of the energy difference between left- and right-handed Weyl points [26]. However, the system remains in the ground state under a static magnetic field, so eventually no actual current should flow [24]. Moreover, detection can be difficult because there is no driving force to induce the current in such an equilibrium state. Hence, instead of a static magnetic field, one should consider a nonequilibrium magnetic field to obtain the net current of the chiral magnetic effect.

Recent studies using femtosecond laser pulses have established a method of generating nonequilibrium magnetic fields using circularly polarized light in ferrimagnets [33–35]. The light-induced effective magnetic field $\boldsymbol{B}^{\text{eff}}$ is given by

$$\boldsymbol{B}^{\text{eff}} \propto i\boldsymbol{\mathcal{E}} \times \boldsymbol{\mathcal{E}}^*, \tag{1}$$

where $\boldsymbol{\mathcal{E}}$ is the circularly polarized complex electric field [36, 37]. The effective magnetic field is generated by the conversion of spin angular momentum from light to electrons via spin–orbit coupling [37–39]. The direction of $\boldsymbol{B}^{\text{eff}}$ depends on the chirality of the circularly polarized light. Its magnitude is proportional to the laser intensity and can reach 20 T for a sufficiently strong laser pulse [33–35].

In this Letter, we theoretically predict a giant current $\boldsymbol{j}$ induced by the effective magnetic field (Fig. 1). The photovoltaic current is due to a nonequilibrium spin distribution near the Fermi surface. For lower-frequency light, the conversion of spin angular momentum between light
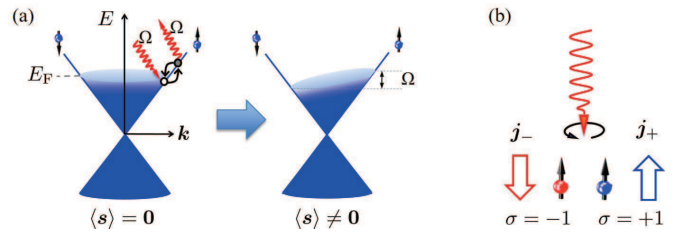
FIG. 1: (Color online) Schematic illustration of photovoltaic chiral magnetic effect: (a) For a lower-frequency light regime, electrons near the Fermi surface are excited by incident light through the Raman process illustrated. As a result, a finite spin distribution is generated near the Fermi surface, and the spin of Weyl fermions is aligned in the direction of the effective magnetic field $\boldsymbol{B}^{\text{eff}}$, on average. (b) For the reason given above, the circularly polarized light aligns the spin of Weyl fermions. Because of (pseudo)spin–momentum locking, Weyl fermions with helicity $\sigma = 1$ ($\sigma = -1$) move in the same (opposite) direction as the spin, which results in nonzero current $\boldsymbol{j}_\sigma$.

and electrons occurs only near the Fermi surface. Thus, the low-energy description using Weyl fermions gives a good approximation for evaluating the photovoltaic current. On the basis of the Keldysh Green function, we show that a net current is obtained by applying circularly polarized light. The current is proportional to the effective magnetic field, in the form of the chiral magnetic effect. On the other hand, unlike other chiral magnetic effects[17–21, 24–27], it is dissipative and extrinsic. For Ta compound Weyl semimetals, the current reaches a huge value of $O(10^6)$ A/m^2.

Model—We consider the following Hamiltonian to describe Weyl–Dirac semimetals in the presence of circularly polarized light:

$$H = H_{\text{Weyl}} + H_{\text{em}} + V_{\text{imp}}. \tag{2}$$

The first term is the Hamiltonian of Weyl–Dirac semimetals. At low energy, it takes the form

$$H_{\text{Weyl}} = \sum_{\boldsymbol{k}} \psi_{\boldsymbol{k}}^{\dagger} \mathcal{H}_{\text{Weyl}} \psi_{\boldsymbol{k}}, \tag{3}$$

$$\mathcal{H}_{\text{Weyl}} = \hbar v_{\text{F}} \sigma^z (\boldsymbol{k} - \sigma^z \boldsymbol{b}) \cdot \boldsymbol{s} - \mu \sigma^0 s^0 - \mu_5 \sigma^z s^0, \tag{4}$$

where $\psi_{\boldsymbol{k}} = {}^t(\psi_{\uparrow,+}\ \psi_{\downarrow,+}\ \psi_{\uparrow,-}\ \psi_{\downarrow,-})$ is the annihilation operator of an electron with (pseudo)spin $(\uparrow,\downarrow)$ and helicity $(+,-)$. Further, s^μ and σ^μ are the Pauli matrices of the (pseudo)spin and helicity, respectively; v_{F} is the Fermi velocity, and μ is the chemical potential. The parameters $2\boldsymbol{b}$ and $2\mu_5$ denote the difference in the positions of left- and right-handed Weyl points in momentum and energy space, respectively. For Dirac semimetals, $\boldsymbol{b} = \boldsymbol{0}$ and $\mu_5 = 0$. The second term in Eq. (3) represents the gauge coupling between Weyl–Dirac semimetals and light:

$$H_{\text{em}} = -\sum_{\boldsymbol{k}} \boldsymbol{j} \cdot \boldsymbol{A}^{\text{em}}, \tag{5}$$

where $\boldsymbol{j}$ denotes the charge current, and $\boldsymbol{A}^{\text{em}}$ is the vector potential of light. For circularly polarized light, the electric field $\boldsymbol{E}^{\text{em}} = -\partial_t \boldsymbol{A}^{\text{em}}$ is given by $\boldsymbol{E}^{\text{em}} = \text{Re}\left[\boldsymbol{\mathcal{E}} e^{i\Omega t}\right]$, where $\boldsymbol{\mathcal{E}}$ is a complex vector, and Ω is the angular frequency of light. The third term in Eq. (2) expresses the impurity scattering in Weyl–Dirac semimetals [40, 41]:

$$V_{\text{imp}} = \sum_{\boldsymbol{k},\boldsymbol{q}} \psi_{\boldsymbol{k}+\boldsymbol{q}}^{\dagger} \sigma^0 s^0 u_{\text{imp}}(\boldsymbol{q}) \psi_{\boldsymbol{k}}. \tag{6}$$

The impurity scattering potential u_{imp} is assumed to be short-ranged and triggers a finite relaxation time, which is given within the Born approximation as $\tau_{\text{e},\sigma} = \hbar/(\pi \nu_{\text{e},\sigma} n_{\text{c}} u_{\text{imp}}^2)$ with a concentration of nonmagnetic impurities n_{c}.

Current induced by circularly polarized light— We calculate the current induced by light using the

Keldysh Green function technique [41]. Below, we assume that $\hbar\Omega$ is much lower than the bandwidth, so the low-energy effective Hamiltonian (3) gives a good approximation. For Eq. (3), the current is defined as $\langle \boldsymbol{j} \rangle \equiv e v_{\text{F}} \langle \psi^{\dagger}(\boldsymbol{x},t) \sigma^z \boldsymbol{s} \psi(\boldsymbol{x},t) \rangle$, which is decomposed as

$$\langle \boldsymbol{j} \rangle \equiv \langle \boldsymbol{j}_+ \rangle + \langle \boldsymbol{j}_- \rangle, \tag{7}$$

where $\langle \boldsymbol{j}_{\sigma=\pm} \rangle \equiv \sigma e v_{\text{F}} \langle \psi_\sigma^{\dagger} \boldsymbol{s} \psi_\sigma \rangle$. Here $\psi_\sigma^{\dagger} = (\psi_{\sigma,\uparrow}^{\dagger}, \psi_{\sigma,\downarrow}^{\dagger})$ is the creation operator of Weyl fermions with helicity $\sigma = \pm$. There is no mixing term between ψ_+ and ψ_- in H; thus, $\langle \boldsymbol{j}_+ \rangle$ and $\langle \boldsymbol{j}_- \rangle$ can be calculated separately. First, we consider the $\boldsymbol{b} = 0$ case.

In terms of the Keldysh Green function, the chiral current $\langle \boldsymbol{j}_\sigma \rangle$ is represented as $\langle \boldsymbol{j}_\sigma \rangle = -\sigma i \hbar e v_{\text{F}} \text{tr}[\boldsymbol{s} G_\sigma^<(\boldsymbol{x},t:\boldsymbol{x},t)]$, where the 2×2 matrix lesser Green function $G_\sigma^<(\boldsymbol{x},t:\boldsymbol{x},t) = -i\hbar \langle \psi_\sigma^{\dagger}(\boldsymbol{x},t) \psi_\sigma(\boldsymbol{x},t) \rangle$. The contribution from $\boldsymbol{B}^{\text{eff}} \propto i\boldsymbol{\mathcal{E}} \times \boldsymbol{\mathcal{E}}^*$ is given by the diagrams in Fig. 2. It is written as

$$\langle j_\sigma^i \rangle = -i\hbar e v_{\text{F}} [\mathcal{I}_\sigma^{ijk}(\Omega) + \mathcal{I}_\sigma^{ijk}(-\Omega)] \mathcal{E}^j \mathcal{E}^{*k}, \tag{8}$$

where $\mathcal{I}_\sigma^{ijk}(\Omega) = \frac{e^2 v_{\text{F}}^2}{4\Omega^2} \sum_{I=a,b,c,d} \mathcal{C}_\sigma^{(I),ijk}$. Each diagram in Fig. 2 gives the following $\mathcal{C}_\sigma^{(I=a,b,c,d),ijk}$:

$$\mathcal{C}_\sigma^{(a),ijk} = \sum_{\boldsymbol{k},\omega} \text{tr}\left[s^i g_{\boldsymbol{k},\omega,\sigma} s^j g_{\boldsymbol{k},\omega+\Omega,\sigma} s^k g_{\boldsymbol{k},\omega,\sigma} \right]^<,$$

$$\mathcal{C}_\sigma^{(b),ijk} = \sum_{\boldsymbol{k},\omega} \text{tr}\left[s^i g_{\boldsymbol{k},\omega,\sigma} \mathcal{S}_{\omega,\omega+\Omega}^j g_{\boldsymbol{k},\omega+\Omega,\sigma} s^k g_{\boldsymbol{k},\omega,\sigma} \right]^<,$$

$$\mathcal{C}_\sigma^{(c),ijk} = \sum_{\boldsymbol{k},\omega} \text{tr}\left[s^i g_{\boldsymbol{k},\omega,\sigma} s^j g_{\boldsymbol{k},\omega+\Omega,\sigma} \mathcal{S}_{\omega+\Omega,\omega}^k g_{\boldsymbol{k},\omega,\sigma} \right]^<,$$

$$\mathcal{C}_\sigma^{(d),ijk} = \sum_{\boldsymbol{k},\omega} \text{tr}\left[\mathcal{S}_{\omega,\omega}^i g_{\boldsymbol{k},\omega,\sigma} s^j g_{\boldsymbol{k},\omega+\Omega,\sigma} s^k g_{\boldsymbol{k},\omega,\sigma} \right]^<, \tag{9}$$

where $g_{\boldsymbol{k},\omega,\sigma}^<$ is given by $g_{\boldsymbol{k},\omega,\sigma}^< = f_\omega[g_{\boldsymbol{k},\omega,\sigma}^{\text{a}} - g_{\boldsymbol{k},\omega,\sigma}^{\text{r}}]$ with the Fermi distribution function f_ω and the advanced and retarded Green's functions as $g_{\boldsymbol{k},\omega,\sigma}^{\text{a}}$ and $g_{\boldsymbol{k},\omega,\sigma}^{\text{r}} = [\hbar\omega - \sigma\hbar v_{\text{F}}\boldsymbol{k} \cdot \boldsymbol{s} + \mu + \sigma\mu_5 + i\hbar/(2\tau_{\text{e},\sigma})]^{-1}$. $\mathcal{S}_{\omega,\omega'}^i$ is the vertex correction because of the nonmagnetic impurity scattering V_{imp} [42].

Using above equations, one can rewrite $\mathcal{C}_\sigma^{(I=a,b,c,d),ijk}$ in terms of the retarded and advanced Green's functions. For $|\mu + \sigma\mu_5| \gg \hbar/\tau_{\text{e}}$, we find that

$$C_\sigma^{(I=a,b,c,d),ijk} \propto \sum_\omega (f_{\omega+\Omega} - f_\omega). \tag{10}$$

This means that only fermions near the Fermi surface contribute to the light-induced current, which justifies our Weyl fermion approximation. We also find that $C_\sigma^{(I),ijk}$ contains both the retarded and advanced Green's functions, and it is expressed as their product. This indicates a nonequilibrium process [41].

After some calculation [42], we obtain

$$\langle \boldsymbol{j}_\sigma \rangle = \sigma \frac{2\nu_{\text{e},\sigma} e^3 v_{\text{F}}^3 \tau_{\text{e},\sigma}^4}{3\hbar} \Omega i(\boldsymbol{\mathcal{E}} \times \boldsymbol{\mathcal{E}}^*), \tag{11}$$
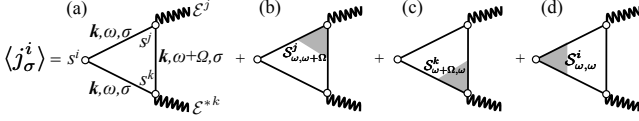
FIG. 2: Diagrammatic representation of a charge current $\langle j_\sigma^i \rangle$ via the photovoltaic chiral magnetic effect (a) without and (b–d) with a vertex correction for nonmagnetic impurity scattering. Wavy lines denote the electric field of the polarized light.

where $\nu_{e,\sigma} = \frac{(\mu + \sigma \mu_5)^2}{2\pi^2 \hbar^3 v_F^3}$ is the density of states of a Weyl cone with helicity σ. From Eq. (11), the total current $\langle \boldsymbol{j} \rangle$ is

$$\langle \boldsymbol{j} \rangle = \frac{2(\nu_{e,+}\tau_{e,+}^4 - \nu_{e,-}\tau_{e,-}^4)e^3 v_F^3}{3\hbar}\Omega i(\boldsymbol{\mathcal{E}} \times \boldsymbol{\mathcal{E}}^*), \quad (12)$$

which is nonzero when $\nu_{e,+}\tau_{e,+}^4 \neq \nu_{e,-}\tau_{e,-}^4$, namely, when $\mu_5 \neq 0$.

The obtained current originates from a nonequilibrium distribution of spin: When one exposes the system to circularly polarized light, the conversion of spin angular momentum between light and electrons occurs because of spin–orbit interaction. As a result, a nonequilibrium spin distribution arises near the Fermi surface [Fig. 1(a)]. For Weyl fermions, because of spin–momentum locking, the nonequilibrium spin distribution gives rise to the current flow [Fig. 1(b)]. Indeed, for Eq. (3), the current operator is essentially the same as the spin operator; thus, from the same calculation, one can show that the circularly polarized light induces a nonzero spin polarization of electrons,

$$\langle \psi_\sigma^\dagger \boldsymbol{s} \psi_\sigma \rangle = \frac{2\nu_{e,\sigma}e^2 v_F^2 \tau_{e,\sigma}^4}{3\hbar}\Omega i(\boldsymbol{\mathcal{E}} \times \boldsymbol{\mathcal{E}}^*), \quad (13)$$

near the Fermi surface.

Because the circularly polarized light induces spin polarization of electrons, it effectively acts as a Zeeman magnetic field near the Fermi surface:

$$\boldsymbol{B}_\sigma^{\text{eff}} \equiv \chi_\sigma \Omega i \boldsymbol{\mathcal{E}} \times \boldsymbol{\mathcal{E}}^* = \sigma_L \chi_\sigma \Omega |\boldsymbol{\mathcal{E}}|^2 \hat{\boldsymbol{q}}, \quad (14)$$

where $\chi_\sigma \equiv \frac{2}{3}\frac{e^2 v_F^2 \tau_{e,\sigma}^4}{g\mu_B \hbar}$. Here $\hat{\boldsymbol{q}}$ is the unit vector in the direction of light propagation, $\sigma_L = \pm 1$ specifies the chirality (clockwise or counterclockwise polarization) of light, g is the Landé factor, and μ_B is the Bohr magneton.

Note that the light-induced current resembles the chiral magnetic effect. In both cases, the current flows in the direction of an applied magnetic or effective magnetic field, and its magnitude is proportional to the difference in chemical potential between left- and right-handed fermions. Indeed, as in our case, spin polarization and spin–momentum locking are essential to obtaining the current in the chiral magnetic effect [18]. Under a static magnetic field, electrons form the Landau

levels. For Weyl fermions, the zeroth Landau level is fully spin-polarized in the direction of the applied magnetic field; thus, the ground state of the system is also spin-polarized. As a result, the current flows because of spin–momentum locking [18]. We dub our light-induced current effect the photovoltaic chiral magnetic effect.

Here we would like to mention that there is an important difference between our photovoltaic chiral magnetic effect and the original one. In the original case, the chiral magnetic effect is caused by a static magnetic field; thus, the resultant current is in equilibrium (and dissipationless). In condensed matter physics, however, an analogous current of Weyl fermions, even if exists, is completely cancelled by other currents in the conduction band [24]. On the other hand, the photovoltaic chiral magnetic effect is due to the time-dependent electric field, so the current is nonequilibrium and dissipative. The current comes only from Weyl fermions near the Fermi surface, so no cancellation occurs.

The effective magnetic field also generates the axial current, which is the difference between charge currents with different helicity: $\langle \boldsymbol{j}_{\text{axial}} \rangle \equiv \langle \boldsymbol{j}_+ \rangle - \langle \boldsymbol{j}_- \rangle = ev_F[\langle \psi_+^\dagger \boldsymbol{s} \psi_+ \rangle + \langle \psi_-^\dagger \boldsymbol{s} \psi_- \rangle]$. As mentioned above, for lower Ω, the system is well described by Weyl fermions; thus, the axial current can also be well-defined. The axial current is nonzero even for Dirac semimetals with $\boldsymbol{b} = \mu_5 = 0$. The axial current can be detected as the total spin polarization by using pump–probe techniques [33].

We can easily generalize the above result for $\langle \boldsymbol{j} \rangle$ with $\boldsymbol{b} \neq 0$. Because $\boldsymbol{b}$ behaves like a static Zeeman field in $\mathcal{H}_{\text{Weyl}}$, it shifts $\langle \psi_\sigma^\dagger \boldsymbol{s} \psi_\sigma \rangle$ by the Pauli paramagnetism. However, $\boldsymbol{b}$ cannot drive a net current because it is static. Moreover, the circularly polarized light affects only electrons near the Fermi surface, the structure of which does not depend on $\boldsymbol{b}$. Therefore, we have the same current $\langle \boldsymbol{j} \rangle$ in Eq. (12) even when $\boldsymbol{b} \neq 0$.

To have a nonzero $\langle \boldsymbol{j} \rangle$, both the inversion and mirror reflection symmetries should be broken: These symmetries flip the chirality of Weyl fermions, so if exist, the current is cancelled between those of left- and right-handed Weyl fermions. Ta compounds [11–14] realize such Weyl semimetals, with an external field or a strain breaking the mirror reflection symmetry. Trigonal Te under pressure is also a candidate material [43]. We estimate the magnitude of $\boldsymbol{B}_\sigma^{\text{eff}}$ and $\langle \boldsymbol{j} \rangle$ using the material parameters for TaAs [44], $v_F = 3 \times 10^5$ m/s, $\tau_e = 4.5 \times 10^{-11}$ s, and $\mu = 11.5$ meV. With a few percent distortion, μ_5 in TaAs[12] is estimated as $\mu_5 \simeq 1$ meV. We find that $|\boldsymbol{B}_{\sigma=\pm}^{\text{eff}}| = (4.3 \mp 2.6) \times 10^{-16}(\frac{\Omega}{[s^{-1}]})(\frac{|\boldsymbol{\mathcal{E}}|^2}{[V^2/m^2]})$ T. For contentious-wave laser with $|\boldsymbol{\mathcal{E}}| = 4$ kV/m and $\Omega = 2.2 \times 10^9$ s^{-1}, $|\boldsymbol{B}_{\sigma=\pm}^{\text{eff}}|$ is 15 ∓ 9 T. As a result, the induced charge current reaches a huge value of $|\langle \boldsymbol{j} \rangle| \simeq 2 \times 10^6$ A/m^2, which is much larger than the anomalous Hall current density due to the chiral anomaly

[45]. This giant current density is caused by the giant magnetic field $\boldsymbol{B}_\sigma^{\text{eff}}$.

Note that $\langle\boldsymbol{j}\rangle$ is distinguished from the longitudinal [40] and transverse charge currents [27–29, 45], as $\langle\boldsymbol{j}\rangle$ is parallel to the light propagation direction, and it flows in the opposite direction when the chirality of the light is reversed. Our photovoltaic effect is also different from conventional photogalvanic effects [46, 47]. Whereas the conventional one is caused by high-frequency light, our obtained effect is realized in a lower-frequency regime. Furthermore, the direction of the conventional photogalvanic current is anisotropic, reflecting the Rashba spin-orbit interaction[46–48]. On the other hand, the current direction of our effect is universally along the light propagation direction.

Floquet state— So far, we have assumed that the frequency Ω of light is much lower than the scale of the bandwidth. Now, we consider the opposite case. In contrast to the lower-Ω case, in which only electrons near the Fermi surface are influenced by light, the higher-frequency light can affect all of the electrons in valence bands.

To consider this situation, we adopt the Floquet method: Because H in Eq. (2) is periodic in t, i.e., $H(t) = H(t + 2\pi/\Omega)$, the wave function of the Schrödinger equation $i\hbar\partial_t\psi(t) = H(t)\psi(t)$ has the form of $\psi(t) = \sum_m \phi_m e^{-i(\varepsilon+m\hbar\Omega)t/\hbar}$, where the summation is taken for all integers m. Substituting this form into the Schrödinger equation, we have the Floquet equation, $\sum_n H_{m,n}\phi_n = (\varepsilon + m\hbar\Omega)\phi_m$, where $H_{m,n} = (\Omega/2\pi)\int_0^{2\pi/\Omega} dt H(t)e^{i(m-n)\Omega t} + m\hbar\Omega\delta_{m,n}$. For the Hamiltonian in Eq. (2), the diagonal term of the Floquet Hamiltonian is given by $H_{m,m} = H_{\text{Weyl}} + V_{\text{imp}} + m\hbar\Omega$, and the off-diagonal ones are $H_{m,m+1} = H_{m+1,m}^\dagger = (\Omega/2\pi)\int_0^{2\pi/\Omega} dt H_{\text{em}}e^{-i\Omega t} = -\frac{iev_\text{F}|\boldsymbol{\mathcal{E}}|}{2\Omega}\sigma^z(s^x - i\sigma_\text{L}s^y)$ when light travels along the z axis. The other off-diagonal terms are identically zero. Each solution of the Floquet equation gives a periodic steady state.

For large Ω, the diagonal terms are dominant, so one can treat the off-diagonal ones as a perturbation. In the zeroth order, our system is described by $H_{0,0} = H_{\text{Weyl}} + V_{\text{imp}}$; then the first nonzero correction in the perturbation theory appears in the second order as $\frac{1}{\hbar\Omega}[H_{0,-1}, H_{0,1}]$. Thus, we obtain the following effective Hamiltonian:

$$H_{\text{eff}} = H_{\text{Weyl}} + V_{\text{imp}} - i\sigma^0\frac{e^2 v_\text{F}^2}{\hbar\Omega^3}(\boldsymbol{\mathcal{E}}\times\boldsymbol{\mathcal{E}}^*)\cdot\boldsymbol{s}, \quad (15)$$

which describes a periodic steady state of our system.

From Eq. (15), it is found that higher-frequency light induces a different effective Zeeman magnetic field,

$$\boldsymbol{B}_{\text{Floquet}}^{\text{eff}} \equiv \frac{e^2 v_\text{F}^2}{g\mu_\text{B}\hbar\Omega^3}i\sigma^0(\boldsymbol{\mathcal{E}}\times\boldsymbol{\mathcal{E}}^*). \quad (16)$$

Here we note that the physical origin is completely different from that in the lower-frequency case. $\boldsymbol{B}_\sigma^{\text{eff}}$ in Eq.

(14) originates from a dissipative process, so it depends on $\tau_{\text{e},\sigma}$; in contrast, $\boldsymbol{B}_{\text{Floquet}}^{\text{eff}}$ in Eq. (16) is independent of the impurity scattering. Furthermore, the former magnetic field affects only electrons near the Fermi surface, but the latter acts on the entire band. Consequently, the resultant phenomena can be different.

We find that no net current $\langle\boldsymbol{j}\rangle$ is produced by $\boldsymbol{B}_{\text{Floquet}}^{\text{eff}}$: According to Eq. (15), $\boldsymbol{B}_{\text{Floquet}}^{\text{eff}}$ provides only a uniform Zeeman splitting (or shift) in the entire spectrum of the band of the Weyl semimetal, like a static Zeeman field. Therefore, in a steady state, electrons fill the band up to the Fermi energy. In this situation, one can use the same argument in Ref. [24] and prove that $\langle\boldsymbol{j}\rangle = 0$. Whereas Weyl fermions may have a nonzero spin $\langle\psi_\sigma^\dagger\boldsymbol{s}\psi_\sigma\rangle$ due to the Pauli magnetism of $\boldsymbol{B}_{\text{Floquet}}^{\text{eff}}$, the current due to spin–momentum locking is totally cancelled by the current from the rest of the band. In other words, no photovoltaic chiral magnetic effect occurs for higher-frequency light.

It is helpful to regard the frequency Ω as an energy cutoff for the chiral magnetic effect. For lower Ω, the light can excite only Weyl fermions near the Fermi surface; thus, quasi-relativistic phenomena such as the chiral magnetic effect may occur. As Ω increases, electrons at a lower position in the band can participate in the current; then, eventually, when Ω is large enough to affect the entire spectrum of the band, the chiral magnetic effect is completely cancelled.

Instead, for higher Ω, one can expect the light-induced anomalous Hall effect. Substituting Eq. (3) for H_{Weyl} in Eq. (15), one finds that $\boldsymbol{B}_{\text{Floquet}}^{\text{eff}}$ shifts $\boldsymbol{b}$ by $\delta\boldsymbol{b} = -(g\mu_\text{B}/2\hbar v_\text{F})\boldsymbol{B}_{\text{Floquet}}^{\text{eff}}$. The change in $\boldsymbol{b}$ induces a change in the θ term in Weyl semimetals [26], which results in $\langle\delta\rho\rangle = \frac{2\alpha c\epsilon_0}{\pi}\delta\boldsymbol{b}\cdot\boldsymbol{B}$ and $\langle\delta\boldsymbol{j}\rangle = -\frac{2\alpha c\epsilon_0}{\pi}\delta\boldsymbol{b}\times\boldsymbol{E}$ in the presence of external magnetic and electric fields $\boldsymbol{B}$ and $\boldsymbol{E}$. Here α is the fine structure constant, c is the speed of light, and ϵ_0 is the vacuum permittivity. The light-induced charge pump $\langle\delta\rho\rangle$ and anomalous Hall current $\langle\delta\boldsymbol{j}\rangle$ were discussed recently in Refs. [49–51].

Conclusion— We theoretically predict the photovoltaic chiral magnetic effect, which is induced by the effective magnetic field due to circularly polarized light. In the low-light-frequency regime, the effective magnetic field affects only fermions near the Fermi surface. As a result, the effective magnetic field triggers a finite spin polarization of Weyl fermions and drives the finite charge current in Eq. (12). On the other hand, in the high-frequency regime, the Floquet quasi-steady state is realized. The circularly polarized light induces the effective magnetic field in Eq. (16), which is completely different from that in the lower-frequency regime. The magnetic field in the high-frequency regime behaves like the Zeeman field and shifts the entire band structure. The current of Weyl fermions is completely cancelled by other band contributions. Our photovoltaic chiral magnetic effect, which depends strongly on the light frequency,

realizes the chiral magnetic effect in condensed matter physics.

Acknowledgments

---

[1] S. Murakami, New J. Phys. **9**, 356 (2007).

[2] B-J. Yang and N. Nagaosa, Nat. Comm. **5**, 4898 (2014).

[3] A. A. Burkov and Leon Balents, Phys. Rev. Lett. **107**, 127205 (2011).

[4] M. Brahlek, N. Bansal, N. Koirala, S. Y. Xu, M. Neupane, C. Liu, M. Z. Hasan, and S. Oh, Phys. Rev. Lett. **109**, 186403 (2012).

[5] L. Wu, M. Brahlek, R. Valdes A., A. V. Stier, C. M. Morris, Y. Lubashevsky, L. S. Bilbro, N. Bansal, S. Oh, and N. P. Armitage, Nature Physics **9**, 410 (2013).

[6] Z. Wang, Y. Sun, X. Q. Chen, C. Franchini, G. Xu, H. Weng, X. Dai, and Z. Fang, Phys. Rev. B **85**, 195320 (2012).

[7] Z. K. Liu, B. Zhou, Y. Zhang, Z. J. Wang, H. M. Weng, D. Prabhakaran, S. K. Mo, Z. X. Shen, Z. Fang, X. Dai, Z. Hussain, and Y. L. Chen, Science **343**, 864 (2014).

[8] Z. K. Liu, J. Jiang, B. Zhou, Z. J. Wang, Y. Zhang, H. M. Weng, D. Prabhakaran, S-K. Mo, H. Peng, P. Dudin, T. Kim, M. Hoesch, Z. Fang, X. Dai, Z. X. Shen, D. L. Feng, Z. Hussain and Y. L. Chen, Nature mat. **13**, 677 (2014).

[9] M. Neupane, S.-Y. Xu, R. Sankar, N. Alidoust, G. Bian, C. Liu, I. Belopolski, T.-R. Chang, H.-T. Jeng, H. Lin, A. Bansil, F. Chou, and M. Z. Hasan, Nat. Commun. **5**, 3786 (2014).

[10] M. Novak, S. Sasaki, K. Segawa, and Y. Ando, Phys. Rev. B 91, 041203 (2015).

[11] S. M. Huang, S. Y. Xu, I. Belopolski, C. C. Lee, G. Chang, B. K. Wang, N. Alidoust, G. Bian, M. Neupane, A. Bansil, H. Lin, and M. Z. Hasan, Nat. Comm. **6**, 7373 (2014).

[12] H. Weng, C. Fang, Z. Fang, B. A. Bernevig, and X. Dai, Phys. Rev. X **5**, 011029 (2015).

[13] S. Y. Xu, I. Belopolski, N. Alidoust, M. Neupane, C. Zhang, R. Sankar, S. M. Huang, C. C. Lee, G. C., B. K. Wang, G. Bian, H. Zheng, D. S. Sanchez, F. Chou, H. Lin, S. Jia, and M. Z. Hasan, Science **349**, 613 (2015).

[14] B. Q. Lv, H. M. Weng, B. B. Fu, X. P. Wang, H. Miao, J. Ma, P. Richard, X. C. Huang, L. X. Zhao, G. F. Chen, Z. Fang, X. Dai, T. Qian, and H. Ding, Phys. Rev. X **5**, 031013 (2015).

[15] J. Tominaga, A. V. Kolobov, P. Fons, T. Nakano, and S. Murakami, Adv. Mater. Interfaces **1**, 1300027 (2014).

[16] H. B. Nielsen and M. Ninomiya, Phys. Lett. B **105.2** 219 (1981).

[17] A. Vilenkin, Phys. Rev. D **22**, 3080 (1980).

[18] D. E. Kharzeev, L. D. McLerran, and H. J. Warringa, Nucl. Phys. A **803**, 227 (2008).

[19] K. Fukushima, D. E. Kharzeev, and H. J. Warringa, Phys. Rev. D **78**, 074033 (2008).

[20] M. A. Metlitski and A. R. Zhitnitsky, Phys. Rev. D **72**, 045011 (2005).

[21] D. Kharzeev, K.Landsteiner, A.Schmitt, H.-U. Yee, *Strongly Interacting Matter in Magnetic Fields* (Springer, New York, 2013), Chap.9.

[22] D. E. Kharzeev, Prog. Part. Nucl. Phys. **75**, 133 (2014).

[23] R. Jackiw and V. A. Kostelecky, Phys. Rev. Lett. **82**, 3572 (1999).

[24] M. M. Vazifeh and M. Franz, Phys. Rev. Lett. **111**, 027201 (2013).

[25] D. T. Son and N. Yamamoto, Phys. Rev. Lett. **109**.181602 (2012)

[26] A. A. Zyuzin and A. A. Burkov, Phys. Rev. B **86**, 115133 (2012).

[27] A. A. Zyuzin, S. Wu, and A. A. Burkov, Phys. Rev. B **85**, 165110 (2012).

[28] Y. Chen, S. Wu, and A. A. Burkov, Phys. Rev. B **88**, 125105 (2013).

[29] A. A. Burkov, J. Phys. Condens. Matter **27**, 113201 (2015).

[30] H. Sumiyoshi and S. Fujimoto, arXiv1509.03981v2.

[31] K. Nomura and D. Kurebayashi, Phys. Rev. Lett. 115, 127201 (2015).

[32] K. Taguchi and Y. Tanaka, Phys. Rev. B **91**, 054422 (2015).

[33] A. Kirilyuk, A. V. Kimel, and T. Rasing, Rev. Mod. Phys. **82**, 2731 (2010).

[34] C. D. Stanciu, F. Hansteen, A. V. Kimel, A. Kirilyuk, A. Tsukamoto, A. Itoh, and T. Rasing, Phys. Rev. Lett. **99**, 047601 (2007).

[35] K. Vahaplar, A. M. Kalashnikova, A. V. Kimel, D. Hinzke, U. Nowak, R. Chantrell, A. Tsukamoto, A. Itoh, A. Kirilyuk, and Th. Rasing, Phys. Rev. Lett. **103**, 117201(2009).

[36] L. P. Pitaevskii, Sov. Phys. JETP **12**, 1008 (1961).

[37] P. S. Pershan, J. P. van der Ziel, and L. D. Malmstrom, Phys. Rev. **143**, 574 (1966).

[38] K. Taguchi and G. Tatara, Phys. Rev. B **84**, 174433 (2011).

[39] T. Misawa, T. Yokoyama, and S. Murakami, Phys. Rev. B. **84**.165407 (2011).

[40] P. Hosur, S. A. Parameswaran, and A. Vishwanath, Phys. Rev. Lett. **108**, 046602 (2012).

[41] H. Haug and A. P. Jauho, *Quantum Kinetics in Transport and Optics of Semiconductors*, 2nd ed. (Springer, New York, 2007).

[42] See the supplemental material for "Photovoltaic Chiral Magnetic Effect".

[43] M. Hirayama, R. Okugawa, S. Ishibashi, S. Murakami, and T. Miyake, Phys. Rev. Lett. 114, 206401 (2015).

[44] C. Zhang, Z. Yuan, S.-Y. Xu, Z. Lin, B. Tong, M. Z. Hasan, J. Wang, C. Zhang, S. Jia, arXiv:1502.00251.

[45] A. Sekine and K. Nomura, arXiv 1508.04590.

[46] S. D. Ganichev and W. Prettl, J. Phys. Condens. Matter **15**, R935 (2003).

[47] J. W. McIver, D. Hsieh, H. Steinberg, P. Jarillo-Herrero, N. Gedik, Nature Nanotech. **7**, 96 (2012).

[48] P. Hosur, Phys. Rev. B **83**, 035309 (2011).

[49] S. Ebihara, K. Fukushima, and T. Oka, arXiv 1509.03673.

[50] C. K. Chan, P. A. Lee, K. S. Burch, J. H. Han, and Y. Ran, Phys. Rev. Lett. **116**, 026805 (2016).

[51] T. Oka and H. Aoki, Phys. Rev. B **79**, 081406(R) (2009).